Electronic Supplementary Material (ESI) for Physical Chemistry Chemical Physics.

ESI of

Role of post-CCSD(T) corrections in predicting the energetics and kinetics of the $OH^{\bullet}+O_3$ reaction

Philips Kumar Rai† and Pradeep Kumar*,‡

†*Department of Chemistry, Malaviya National Institute of Technology Jaipur, Jaipur, 302017,India*

‡*Department of Chemistry, Malaviya National Institute of Technology Jaipur, Jaipur, 302017, India*

E-mail: pradeep.chy@mnit.ac.in

Sl. No. **Contents**

Table S1: Cartesian coordinates and all normal mode frequencies of the optimized geometries calculated at CASPT2/aug-cc-pVTZ level of theory.

Compound	Cartesian coordinate (Å)				Frequencies (cm^{-1})		
$OH^{\bullet}$ (3,3)	O	0.00000000	0.00000000	0.05956815		4133.48	
	H	0.00000000	0.00000000	-0.91038715			
O_3 (8,7)	O	0.00000000	-0.00304975	0.44068792			
	O	0.00000000	1.08828425	-0.22126828	716.11	1020.39	1198.93
	O	0.00000000	-1.08523450	-0.21941864			
RC (11,10)	O	-1.18878945	0.68196522	-0.00000107			
	O	0.00200993	1.14883152	0.00000458	33.99	59.68	95.60
	O	-1.29646118	-0.58702928	0.00000088	191.13	327.33	721.91
	H	1.51983757	-0.55667737	-0.00001398	1127.57	1141.24	3731.88
	O	2.30995913	-1.12566109	0.00000958			
TS1 (11,10)	O	-1.725945	-0.581505	-0.182093			
	O	-1.071382	0.525144	-0.254833	-444.42	116.86	193.40
	O	-0.032987	0.602238	0.518695	268.30	599.68	694.77
	O	1.341055	-0.639776	-0.373902	814.79	1028.83	3641.00
	H	1.169952	-1.327934	0.289963			
TS2 (11,10)	O	-1.88938947	-0.47074821	-0.15719146			
	O	-1.05325549	0.48939150	-0.31479741	-442.96	107.70	196.46
	O	-0.06308422	0.49675970	0.53351412	243.34	612.73	700.81
	O	1.38453313	-0.63208574	-0.37748813	890.50	1103.76	3558.88

	H	1.95649785	0.14641084	-0.44467326			
$HO_2^\bullet$ (3,3)	O	0.62734546	-0.07267995	0.00000000	1135.25	1460.02	3687.34
	O	-0.68366579	0.01649025	0.00000000			
	H	0.94000433	0.84778170	0.00000000			
O_2 (8,7)	O	0.00000000	0.00000000	-0.60640134	1562.05		
	O	0.00000000	0.00000000	0.60640134			

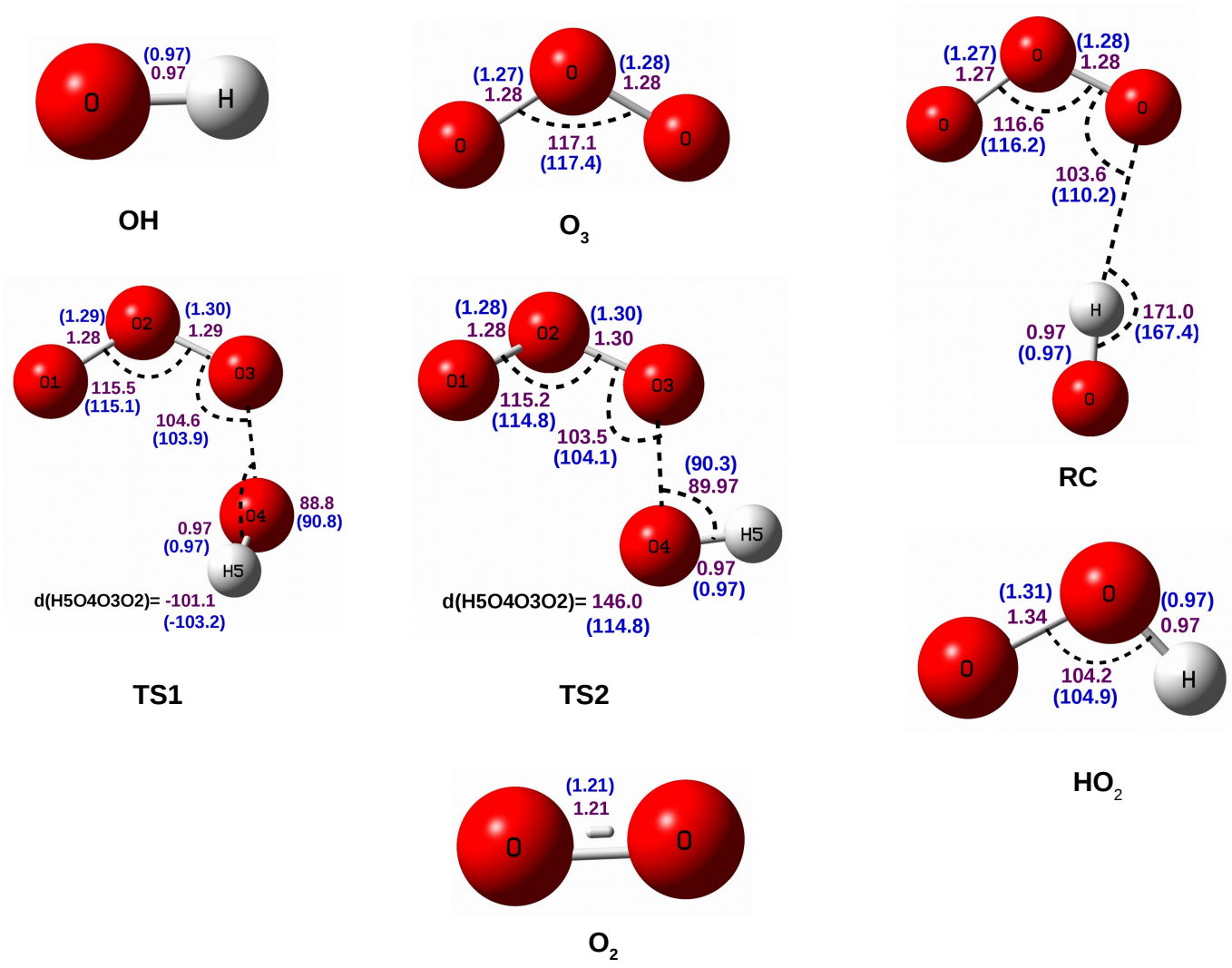

Figure S1: Comparison of the geometrical parameters of all the species involved in the present work obtained at CASPT2/aug-cc-pVTZ level of theory (values given in paranthesis) with the geometrical parameters obtained at CCSD(T)/aug-cc-pVTZ level of theory. The bond-lengths are in Angstrom and bond angles are in degree.

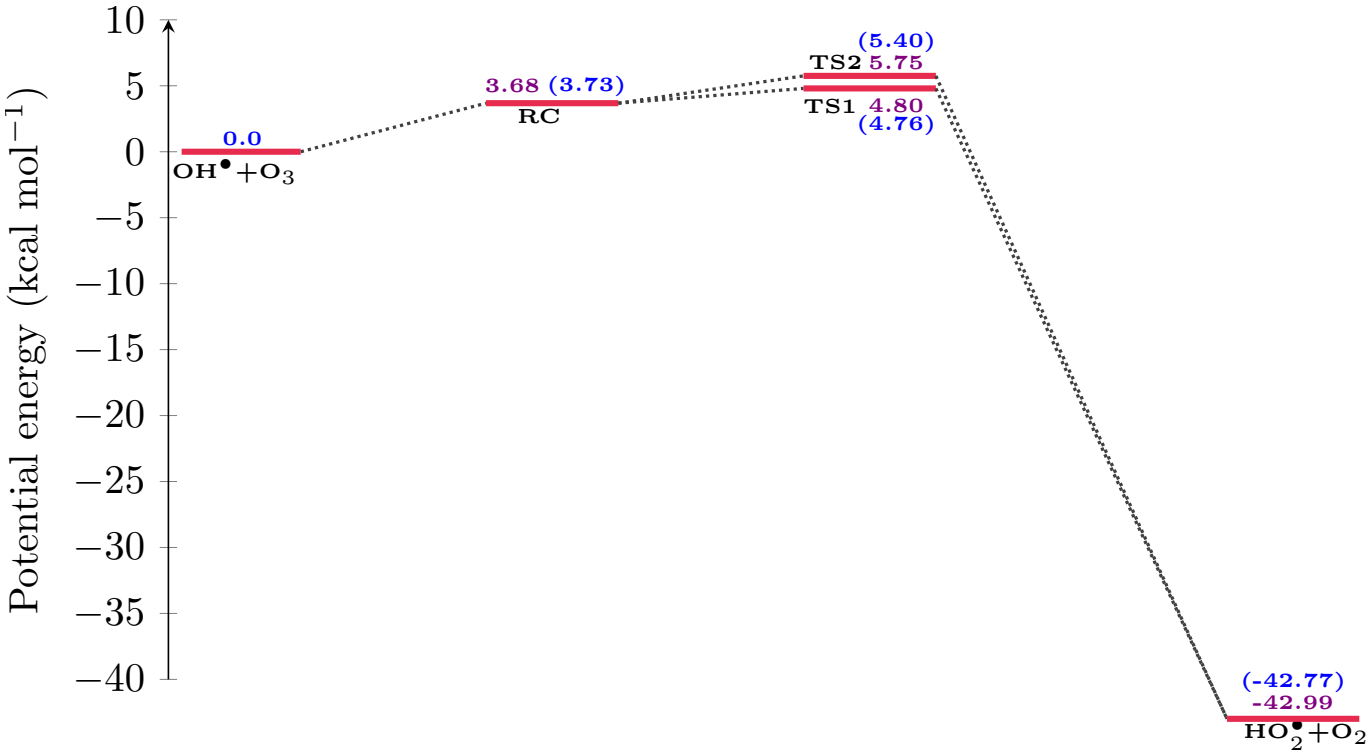

Figure S2: Comparison of the potential energy surface for $OH^{\bullet}+O_3$ reaction obtained by full optimization at CCSD(T)/aug-cc-pVTZ level of theory with the potential energies estimated at CCSD(T)/aug-cc-pVTZ//CASPT2/aug-cc-pVTZ level of theory (values given in paranthesis). The energies are in kcal mol^{-1}.

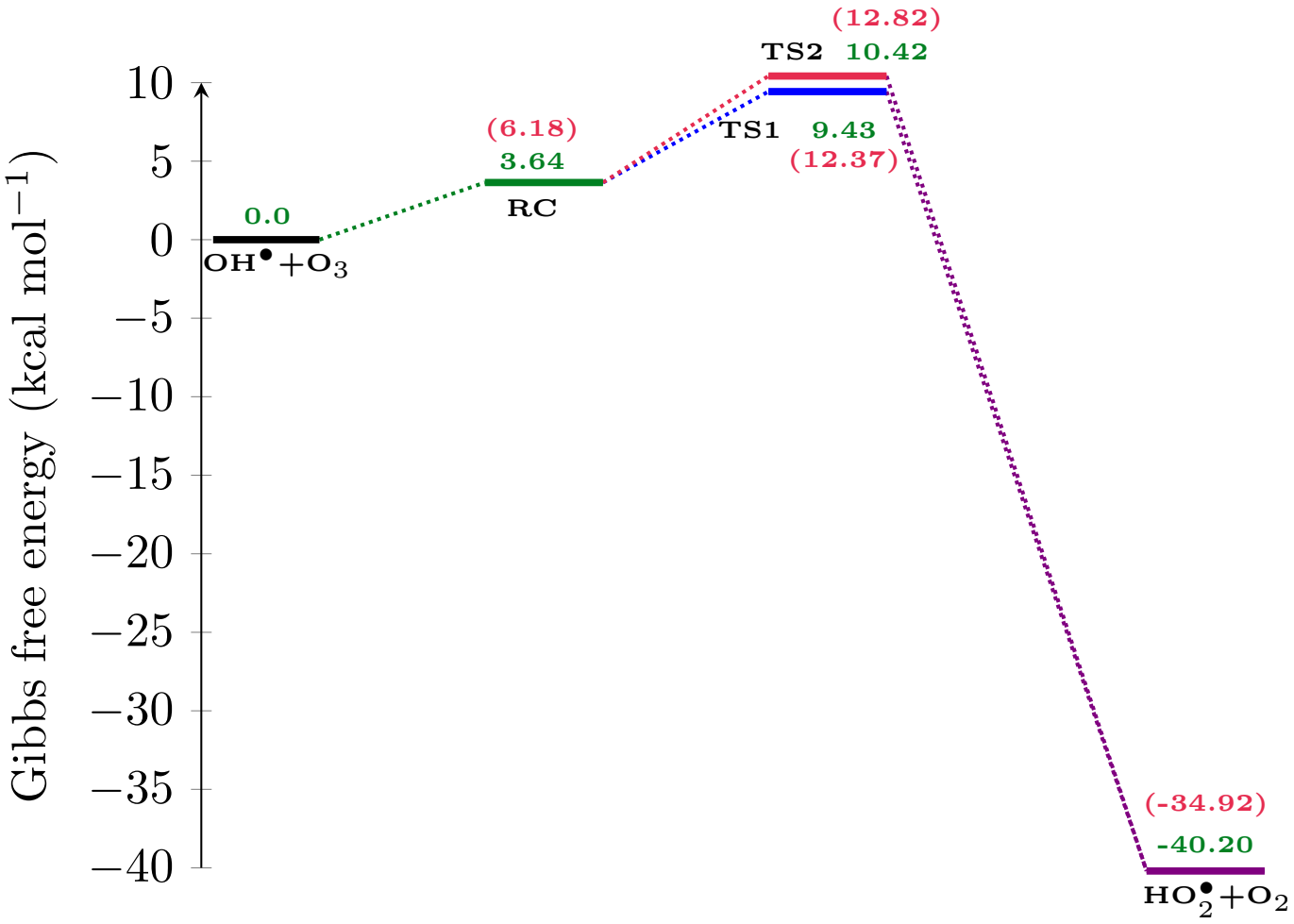

Figure S3: Gibbs free energy profile for the $OH^{\bullet}+O_3$ reaction at 298 K including post-CCSD(T) corrections. The values given in paranthesis are energy obtained at CASPT2/aug-cc-pVTZ level of theory.

Formal proof for an equivalence of rate constants using pre-equilibrium approximation and direct TST calculations:

Pre-equilibrium approximation:

$$OH^{\bullet} + O_3 \xrightarrow{k_{eq}} RC \xrightarrow{k_{uni}} TS \rightarrow HO_2^{\bullet} + O_2 \tag{R1}$$

If the time scale of first step of reaction R1, i.e., $OH^{\bullet}+O_3 \rightarrow RC$, is much much faster than the unimolecular step, then for the reaction R1, the overall bimolecular rate constant (k_{bi}), can be expressed as the product of the k_{eq} and k_{uni}, i.e.,

$$k_{bi} = k_{eq} * k_{uni} \tag{1}$$

Here, the equilibrium constant (k_{eq}) between the isolated reactants and reactant-complex can be computed as:

$$k_{eq} = \frac{Q_{RC}}{Q_{OH\bullet} Q_{O_3}} exp[\frac{-(E_{RC} - E_R)}{RT}] \tag{2}$$

Where, variable Q denote the overall partition functions for the subscripted species $OH^{\bullet}$, O_3 and reactant-complex RC. E_{RC} and E_R symbolise energies of reactant-complex and isolated reactants respectively. On the other hand, the unimolecular rate constants between the reactant-complex and transition state, k_{uni} can be calculated using the following equation:

$$k_{uni} = \frac{k_B T}{h} \frac{Q_{TS}}{Q_{RC}} exp[\frac{-(E_{TS} - E_{RC})}{RT}] \tag{3}$$

Here, k_B; Boltzmann constant, h; Planck's constant and T; Temperature

Hence, using equation (1), (2) and (3);

$$k_{bi} = \frac{k_B T}{h} \frac{Q_{TS}}{Q_{OH\bullet} Q_{O_3}} exp[\frac{-(E_{TS} - E_R)}{RT}] \tag{4}$$

Direct TST:

$$OH^{\bullet} + O_3 \xrightarrow{k_{bi}} TS \rightarrow HO_2^{\bullet} + O_2 \quad \text{(R2)}$$

The bimolecular rate constant (k_{bi}) using direct transition state theory (TST) can be obtained as:

$$k_{bi} = \frac{k_B T}{h} \frac{Q_{TS}}{Q_{OH\bullet} Q_{O_3}} exp[\frac{-(E_{TS} - E_R)}{RT}] \quad (5)$$

Therefore, it is evident from equation (4) and (5) that rate constants obtained by these two methods are identical. A slight variation on the values of rate constant in this article between these two methods of evaluation can be attributed to the difference between their zero curvature tunneling contributions (ZCT). The rate constant values obtained using pre-equilibrium approximation and TST along with their corresponding ZCT contributions are shown in table S2 and S3 respectively of this ESI.

Table S2: The rate constant evaluation (in cm^3 $molecule^{-1}$ s^{-1}) using pre-equilibrium approximation along with their corresponding ZCT contributions.

Temperature (K)	k_{eq}	TS1				TS2			
		k_{TST}	$(k_{PEA})_{TST}$	ZCT	$(k_{PEA})_{TST/ZCT}$	k_{TST}	$(k_{PEA})_{TST}$	ZCT	$(k_{PEA})_{TST/ZCT}$
220	2.58×10^{-22}	5.21×10^{07}	1.34×10^{-14}	1.39	1.87×10^{-14}	5.20×10^{06}	1.34×10^{-15}	1.41	1.90×10^{-15}
225	2.38×10^{-22}	6.14×10^{07}	1.46×10^{-14}	1.37	2.01×10^{-14}	6.48×10^{06}	1.54×10^{-15}	1.39	2.14×10^{-15}
250	1.68×10^{-22}	1.26×10^{08}	2.13×10^{-14}	1.29	2.74×10^{-14}	1.69×10^{07}	2.84×10^{-15}	1.30	3.70×10^{-15}
275	1.29×10^{-22}	2.28×10^{08}	2.93×10^{-14}	1.23	3.61×10^{-14}	3.69×10^{07}	4.75×10^{-15}	1.24	5.90×10^{-15}
298	1.06×10^{-22}	3.58×10^{08}	3.81×10^{-14}	1.19	4.54×10^{-14}	6.72×10^{07}	7.15×10^{-15}	1.20	8.59×10^{-15}
300	1.05×10^{-22}	3.71×10^{08}	3.89×10^{-14}	1.19	4.63×10^{-14}	7.05×10^{07}	7.39×10^{-15}	1.20	8.86×10^{-15}
325	8.92×10^{-23}	5.60×10^{08}	5.00×10^{-14}	1.16	5.80×10^{-14}	1.22×10^{08}	1.09×10^{-14}	1.17	1.27×10^{-14}
350	7.86×10^{-23}	7.97×10^{08}	6.26×10^{-14}	1.14	7.12×10^{-14}	1.95×10^{08}	1.53×10^{-14}	1.14	1.74×10^{-14}
375	7.12×10^{-23}	1.08×10^{09}	7.70×10^{-14}	1.12	8.61×10^{-14}	2.92×10^{08}	2.08×10^{-14}	1.12	2.33×10^{-14}
400	6.59×10^{-23}	1.41×10^{09}	9.31×10^{-14}	1.10	1.03×10^{-13}	4.15×10^{08}	2.74×10^{-14}	1.11	3.03×10^{-14}
425	6.20×10^{-23}	1.79×10^{09}	1.11×10^{-13}	1.09	1.21×10^{-13}	5.67×10^{08}	3.52×10^{-14}	1.09	3.85×10^{-14}
450	5.92×10^{-23}	2.21×10^{09}	1.31×10^{-13}	1.08	1.41×10^{-13}	7.48×10^{08}	4.43×10^{-14}	1.08	4.80×10^{-14}

Table S3: The rate constant evaluation (cm^3 $molecule^{-1}$ s^{-1}) using TST approach along with their corresponding ZCT contributions.

Temperature (K)	TS1			TS2		
	$(k_{bi})_{TST}$	ZCT	$(k_{bi})_{TST/ZCT}$	$(k_{bi})_{TST}$	ZCT	$(k_{bi})_{TST/ZCT}$
220	1.45×10^{-14}	1.45	2.10×10^{-14}	1.45×10^{-15}	1.47	2.13×10^{-15}
225	1.57×10^{-14}	1.42	2.24×10^{-14}	1.66×10^{-15}	1.44	2.39×10^{-15}
250	2.27×10^{-14}	1.33	3.03×10^{-14}	3.03×10^{-15}	1.34	4.07×10^{-15}
275	3.12×10^{-14}	1.27	3.95×10^{-14}	5.05×10^{-15}	1.27	6.43×10^{-15}
298	4.03×10^{-14}	1.22	4.92×10^{-14}	7.57×10^{-15}	1.23	9.28×10^{-15}
300	4.11×10^{-14}	1.22	5.01×10^{-14}	7.82×10^{-15}	1.22	9.56×10^{-15}
325	5.26×10^{-14}	1.18	6.23×10^{-14}	1.14×10^{-14}	1.19	1.36×10^{-14}
350	6.58×10^{-14}	1.16	7.60×10^{-14}	1.60×10^{-14}	1.16	1.86×10^{-14}
375	8.06×10^{-14}	1.13	9.14×10^{-14}	2.17×10^{-14}	1.14	2.47×10^{-14}
400	9.72×10^{-14}	1.12	1.09×10^{-13}	2.85×10^{-14}	1.12	3.19×10^{-14}
425	1.16×10^{-13}	1.10	1.27×10^{-13}	3.66×10^{-14}	1.10	4.04×10^{-14}
450	1.34×10^{-13}	1.09	1.48×10^{-13}	4.60×10^{-14}	1.09	5.03×10^{-14}

Table S4: The unimolecular TST and CVT rate constants (s^{-1}) through TS1 along with their corresponding ZCT and SCT contributions obtained at MN15L/aug-cc-pVTZ level of theory.

T (K)	TST	CVT	ZCT	SCT
220	2.16E+00	1.81E+00	1.025	1.025
225	2.40E+00	2.01E+00	1.023	1.024
250	3.81E+00	3.20E+00	1.019	1.020
275	5.60E+00	4.70E+00	1.016	1.016
298	7.56E+00	6.34E+00	1.013	1.014
300	7.74E+00	6.50E+00	1.013	1.014
325	1.02E+01	8.59E+00	1.011	1.012
350	1.31E+01	1.09E+01	1.010	1.010
375	1.62E+01	1.35E+01	1.008	1.009
400	1.96E+01	1.64E+01	1.007	1.008
425	2.33E+01	1.94E+01	1.007	1.007
450	2.72E+01	2.25E+01	1.006	1.006

Kinetic study of the title reaction using the hindered rotor treatment

Figure S1 shows that both the transition states; TS1 and TS2 can be connected by the rotation of the moiety O-H along the bond axis O-O. Therefore, we have applied the hindered rotor approximation to study the kinetics of this reaction. To compute the hindered rotor partition functions, one need to solve the Time-Independent Schrodinger Equation (TISE) with the hindered rotor potentials. To estimate the hindered rotor potentials, we have scanned along the dihedral angle (H5O4O3O2) for TS1 (figure S1) at CCSD(T)/CBS level of theory (Figure S4). These potential points were used to compute the hindered rotor partition functions by solving the TISE numerically as implemented in MESMER software package.

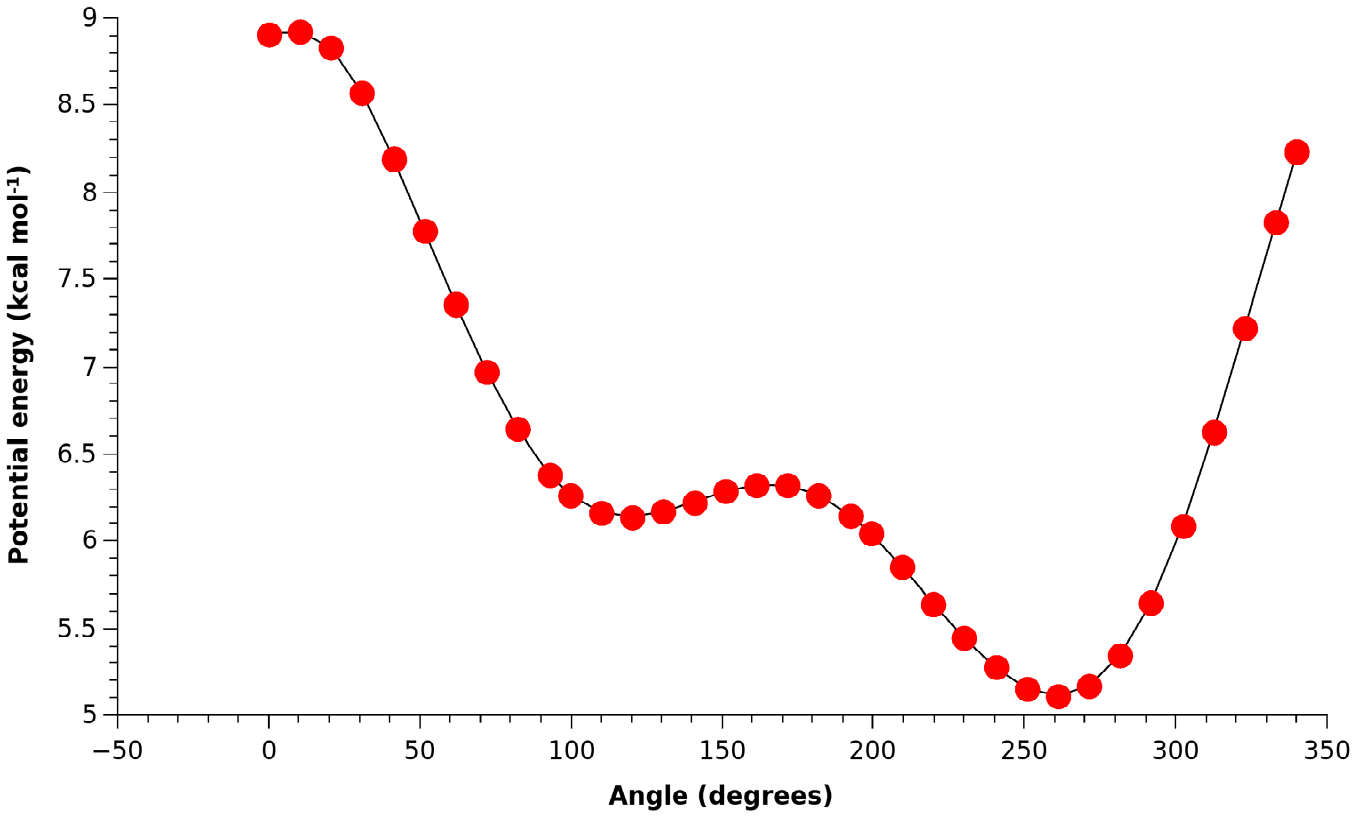

Figure S4: The hindered rotor potentials for TS1 along the internal rotation of O-H moiety obtained at CCSD(T)/CBS level of theory.

Table S5: The bimolecular rate constants estimation using ΔE=126.23 cm^{-1} (k_1) and ΔE=139.21 cm^{-1} (k_2) for OH in cm^3 $molecule^{-1}$ s^{-1} obtained at TST/ZCT method.

T(K)	k_1	k_2
220	2.32E-14	2.26E-14
225	2.48E-14	2.43E-14
250	3.43E-14	3.37E-14
275	4.59E-14	4.52E-14
298	5.85E-14	5.77E-14
300	5.97E-14	5.89E-14
325	7.59E-14	7.50E-14
350	9.46E-14	9.36E-14
375	1.16E-13	1.15E-13
400	1.40E-13	1.39E-13
425	1.68E-13	1.67E-13
450	1.99E-13	1.97E-13